3D atomic structure of nanoscale materials by total x-ray scattering

V. Petkov

Dept. Physics, Central Michigan University, Mt. Pleasant, MI, USA, petkov@phy.cmich.edu

ABSTRACT

Knowledge of the 3D atomic structure is an important prerequisite to understanding, predicting and improving properties of materials. With crystals it is routinely obtained by Bragg x-ray diffraction. Materials structured at the nanoscale, however, lack the extended order of usual crystals rendering traditional crystallography useless. Here we show how a non-traditional approach involving total x-ray scattering and atomic Pair Distribution Function analysis can be used to determine the 3D structure of nanoscale materials in detail. The great potential of the approach is illustrated with examples from recent studies on nanoparticles, nanotubes and polymeric nanotemplates.

Keywords: nanoscale characterization, x-ray scattering

1. INTRODUCTION

X-ray diffraction has long been used to determine the 3D atomic structure of materials. The technique is based on the fact that the wavelength of x-rays is comparable in size to the distances between atoms in most materials. So that when a material in which atoms are ordered over long-range distances, such as a crystal, is irradiated with x-rays it acts as a diffraction grating, and produces a diffraction pattern showing numerous sharp spots, called Bragg diffraction peaks. By measuring and analyzing the peaks it is possible to determine the spatial characteristics of the grating itself – i.e. to determine the 3D atomic arrangement in crystals. This is the essence of the so-called "crystal structure" determination by x-ray diffraction (XRD) [1]. X-ray diffraction has been successfully applied to study the 3D atomic structure of non-crystalline materials (e.g. glasses and liquids) as well. Atoms in non-crystalline materials are ordered over very short distances, usually less than a nanometer, and hardly act as a diffraction grating when irradiated with x-rays. As a result, the XRD patterns of non-crystals are very diffuse in nature and do not show sharp peaks at all. A specialized data analysis approach, known as the atomic Pair Distribution Function (PDF) analysis, has been introduced to study diffuse (non-Bragg type) XRD patterns and extract important structural information about non-crystals such as near atomic neighbor separations and coordination numbers [2]. Thus x-ray diffraction has turned into a valuable research tool in science and technology of both crystalline and non-crystalline materials. Recent rapid development of nanoscience and technology, however, has posed new challenges to the 3D structure determination. With respect to their atomic ordering materials structured at the nanoscale, hereafter called "nanocrystals", are somewhere in between crystals and glasses. Atoms in nanocrystals are ordered over distances of approximately one to a few nanometers and act as a diffraction grating of a very limited yet quantifiable coherence when irradiated with x-rays. As a result, the XRD patterns of nanocrystals show both Bragg-like peaks and a diffuse component (see Fig. 1). The peaks are, however, not as sharp and not as many as observed in the XRD patterns of crystals. Also, the diffuse component is almost as strong as observed in the XRD patterns of non-crystals and may not be neglected. This renders the traditional (Bragg) x-ray crystallography useless. As we demonstrate, the problem may be solved by applying a non-traditional approach based on total x-ray scattering coupled to atomic Pair Distribution Function (PDF) analysis.

2. TOTAL XRD and PDFs: Basics

The frequently used reduced atomic PDF, G(r), gives the number of atoms in a spherical shell of unit thickness at a distance r from a reference atom as follows:

$$G(r) = 4\pi r[\rho(r) - \rho_o] \quad (1)$$

where $\rho(r)$ and ρ_o are the local and average atomic number densities, respectively and r is the radial distance. As defined, the PDF G(r) is a one-dimensional function that oscillates around zero and shows positive peaks at distances separating pairs of atoms, i.e. where the local atomic density exceeds the average one. The negative valleys in the PDF correspond to real space vectors not having atoms at either of their ends. With this respect the PDF resembles the so-called Patterson function that is widely used in traditional x-ray crystallography [1]. However, while the Paterson function is discrete and peaks at interatomic distances within the unit cell of a crystal, the atomic PDF is a continuous function peaking at all interatomc distances occurring in a material. This is an important advantage when the atomic ordering and/or periodicity in materials are substantially limited as in "nanocrystals". The PDF G(r) is the Fourier transform of the experimentally observable total structure function, S(Q), i.e.

$$G(r) = (2/\pi) \int_{Q=o}^{Q_{max}} Q[S(Q) - 1]\sin(Qr)dQ, \quad (2)$$

where Q is the magnitude of the wave vector ($Q=4\pi\sin\theta/\lambda$), 2θ is the angle between the incoming and outgoing x-rays

and λ is the wavelength of the x-rays used [2]. X-ray diffraction usually employs the so-called Faber-Ziman type structure function, S(Q), related to the coherent part of the diffraction pattern, $I^{coh.}(Q)$, as follows:

$$S(Q)=1+\left[I^{coh.}(Q)-\sum c_i \left| f_i\ (Q)\right|^2 \right] / \left| \sum c_i\, f_i(Q) \right|^2, \quad (3)$$

where c_i and $f_i(Q)$ are the atomic concentration and x-ray scattering factor respectively for the atomic species of type *i* [2,3]. As can be seen from Eqs. (1-3), G(r) is simply another representation of the experimental XRD data. However, exploring the diffraction data in real space is advantageous, especially in the case of nanocrystals. First, as Eq. 3 implies the *total* x-ray scattering, including Bragg-like peaks as well as diffuse (non-Bragg-like) scattering, contributes to the PDF. In this way both the measurable atomic order, manifested in the Bragg-like peaks, and all structural "imperfections" that are responsible for its limited (nanoscale) extent, manifested in the intense diffuse component of the diffraction pattern, are reflected in the experimental PDF. Second, by accessing high values of Q, experimental G(r)s of improved real-space resolution [4] can be obtained and, hence, quite fine details in the atomic-scale structure revealed. In fact data at high Q values (Q>10 $Å^{-1}$) are critical to the success of PDF analysis. Diffraction data at high wave vectors are easily obtained using x-rays of a shorter wavelength, i.e. of higher energy. In laboratory conditions such x-rays are produced by standard x-ray tubes with a Mo or Ag anode; modern sources of high-energy x-rays such as synchrotrons may also be employed. And third, G(r) is barely influenced by diffraction optics and experimental factors since these are accounted for in the step of extracting the coherent intensities from the total XRD data (see *Eq.* 3). This makes the PDF an experimental quantity that gives directly relative positions of atoms enabling a convenient determination of important structural parameters (e.g. coordination numbers and distances) as well as testing and refinement of 3D structure models.

3. TOTAL XRD and PDFs: Experimental

Total scattering experiments were carried out at the Advanced Photon Source, Argonne National Laboratory, using x-rays of energy ~ 80-100 keV (λ ~ 0.1 Å). Representative experimental XRD patterns are shown in Fig. 1. As can be seen the XRD pattern of bulk Au shows numerous sharp Bragg peaks to wave vectors as high as 15 $Å^{-1}$, as might be expected for a material exhibiting a long-range, periodic atomic order. Such a diffraction pattern may be analyzed in the traditional crystallographic way, employing Rietveld method for example [5]. The XRD patterns of Au nanoparticles, however, show only a few broad Bragg-like peaks that merge into a slow-oscillating diffuse component already at Q-values as low as 8 $Å^{-1}$ and may not be analyzed in the traditional way easily. Experimental PDFs, derived from the XRD patterns with the help of the program RAD [6], are shown in Fig. 2.

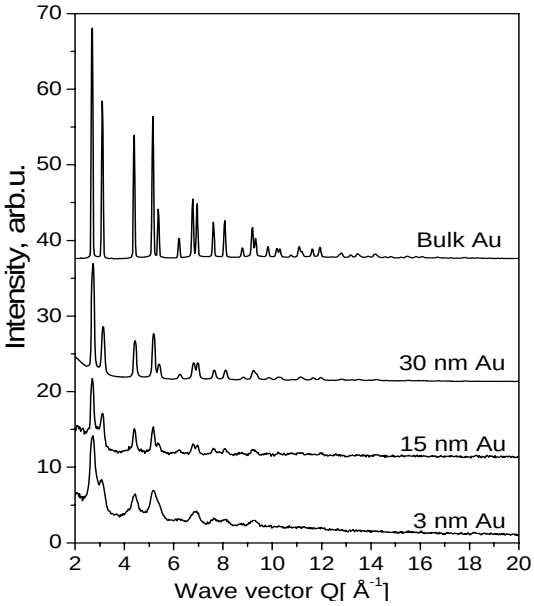

Figure 1: XRD patterns of bulk and nanostructured Au

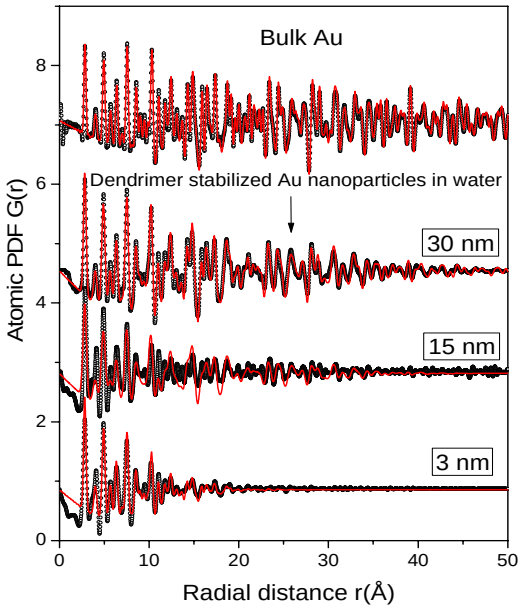

Figure 2: Experimental (symbols) and model (solid red line) PDFs for bulk Au and 3, 15 and 30 nm Au particles

They exhibit several sharp, structure-related features and thus provide a firm basis for an unequivocal 3D structure search and refinement. For example, the first peak in all experimental PDFs is positioned at approx. 2.86(2) Å which is the shortest Au-Au distance in metallic Au. Also, all PDF peaks appear in a sequence found in the fcc-type structure, indicating that all Au samples studied adopt it. However, in contrast to bulk Au crystal, the fcc-type atomic ordering in the nanoparticles is not quite perfect and extends only over distances of 1-3 nm, as indicated by the very rapid decay of the experimental PDFs to zero.

4. Total XRD and PDFs: Examples

4.1 Metallic nanoparticles: Gold

Gold nanoparticles show great promise for applications in selective biological detection, optoelectronics, drug delivery and catalysis. Further improvement of these useful properties requires very good knowledge of the nanoparticle atomic structure. We constructed 3D models for 3, 15 and 30 nm Au particles by quantum Monte Carlo simulations verified by the experimental atomic PDFs, shown in Fig. 2. Our studies [7] find that larger Au nanoparticles (15 and 30 nm) possess a well-defined atomic arrangement of the face-centered-cubic (fcc)-type occurring in bulk gold crystals, with some structural disorder. As such, those nanoparticles may be very well described by crystallographic-type structure models based on fragments of a fcc-type, somewhat distorted but continuous lattice. The fcc-type atomic arrangement in 3 nm Au particles, however, may not be described in terms of a continuous lattice-type model. It may be described by a non-periodic, multiatomic configuration of the type usually employed in structure studies of metallic glasses, such as the one shown in Fig. 3. This finding is in line with previous observations that the

Figure 3: Arrangement of atoms in 3 nm Au particles. The particles appear with a moderately relaxed surface and a more densely packed interior/core divided into domains that are misoriented with respect to each other.

degree of atomic ordering in metallic nanoparticles scales with their size. It should be noted that the computer generated and experimentally (XRD & PDF) verified structure models provide the positions of all atoms inside Au nanopartciles, making possible to compute/predict their structure sensitive properties [8]. This is an important advantage over traditional imaging techniques such as TEM and AFM which yield only a quantitative picture of the nanoparticle structure (surface) projected down one axis.

4.2 Nanotubes: V_2O_5

Crystalline vanadium pentoxide, V_2O_5, is an important technological material widely used in applications such as optical switches, chemical sensors, catalysts and solid-state batteries. The material possesses an outstanding structural versatility and can be manufactured into nanotubes that have many of the useful physicochemical properties of the parent crystal significantly enhanced. For example, the high specific surface area of the nanotubes renders them even more attractive as positive electrodes in secondary Li batteries. Also, the nanotubes show significantly increased capability for redox reactions. The tubes are usually several μm long and have inner diameters between 5 and 15 nm, while the outer diameters range from 15 to 100 nm; their walls consist of several vanadium oxide layers (see Fig. 4). Our total XRD and PDF studies show that even a "nanocrystal" with the complex morphology of V_2O_5 nanotubes possesses an atomic arrangement very well defined on the nanometer length scale that may be described well in terms of a unit cell and symmetry [8]. The unit cell is of triclinic ($P\bar{1}$) symmetry, dimensions of approximately 6 × 6 × 19 Å, and contains only 46 atoms. Knowledge the repetitive structural unit of the tube walls allows to construct a real-size model explaining the unusual tube morphology and, hence, properties. A real-size model of V_2O_5 nanotubes (~ 33,000 atoms in total) is shown in Fig.

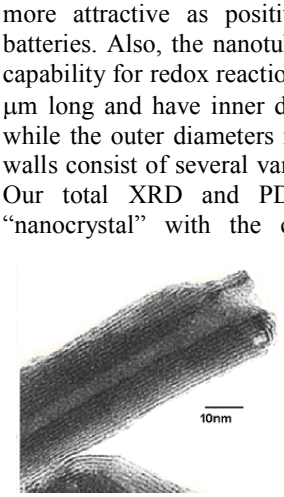

Figure 4: TEM image of V_2O_5 nanotubes

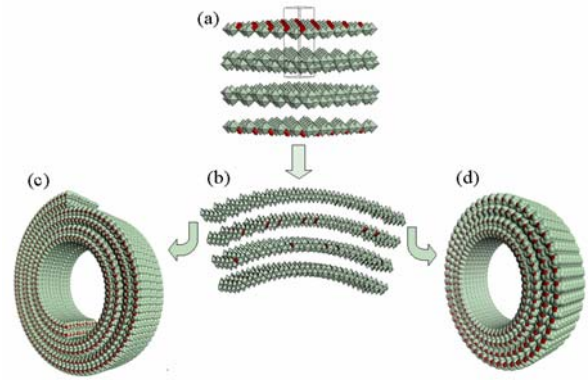

Figure 5: Structure of V_2O_5 nanotubes: double layers of V-O_6 octahedral (light green) and V-O_4 tetrahedral (red) units are almost undistorted and stacked in perfect registry at short distances (a). When bent (b) such layers may form nanoscrolls (c) or closed nanotubes (d).

5. We find that the atomic-scale structure indeed plays an important role in determining the morphology of nanocrystals. Carbon nanotubes are built of graphitic sheets one atomic layer thin that is flexible enough to bend into tubes of diameter of 1 nm. Vanadium pentoxide nanotubes are build of thick layers of much more complex structure (see Fig. 5) that can only be accommodated in nanotubes of diameters of 5 nm or larger, as observed in practice.

4.3 Macromolecular templates: PAMAM dendrimers

Dendrimers are a novel class of structurally controlled macromolecules derived through a so-called "branches-upon-branches" growing process. Dendrimers can be designed with a variety of organic and inorganic cores and branches, with tunable branch length, multiplicity, and surface functionality. The ability to control the structure at this level has created substantial interest in the use of dendrimers as templates for multifunctional nanocomposites [10]. The concept of an empty interior is central to the understanding of important properties of dendrimers, in particular their ability to host nanosize objects. We used total XRD and the PDF approach to determine the atomic arrangement in dendrimeric poly(amidoamine) (PAMAM) macromolecules [11].

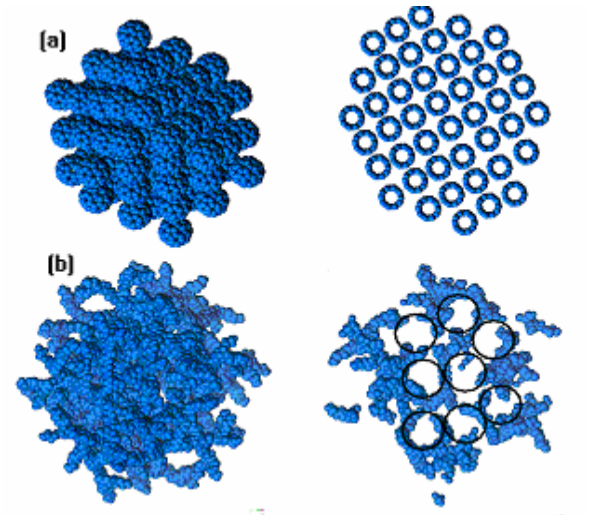

Figure 6: 3D models (on the left) for (a) fullerene C_{60} and (b) PAMAM dendrimer. Slices cut trough the central part of the models are shown on the right. Fullerene is a fcc-type arrangement of rigid C_{60} molecules/spheres, each 0.7 nm Å in diameter. PAMAM dendrimers show a branched-type structure with cavities (big open circles) that are approximately 1 nm in diameter.

Analysis of the 3D structure models, shown in Fig. 6, allows to draw important conclusions about the atomic arrangement in dendrimers. Higher-generation PAMAMs are globular in shape and with a relatively open internal structure. The polymeric branches inside dendrimers are arranged in a semi-regular pattern forming a network-like structure. This branched network supports cavities with a narrowly distributed diameters ranging from 0.5 to 1.5 nm (see Fig. 6b). The cavities occur throughout the interior of the macromolecules and are joined into channels connecting the molecule surface and core. Due to their unique 3D structure PAMAM dendrimers can accommodate small (~ 1nm) guest molecules and clusters, providing them with a unique nanoenvironment.

5. CONCLUSION

Using total x-ray scattering and PDF data analysis we have determined the atomic structure of three distinct types of "nanocrystals". We have also successfully determined the 3D structure of other nanoscale materials of key technological importance such as nanoceramics [12], nanosheets [13] and nanomagnets [14]. The marked flexibility with respect to sample's state, morphology, amount and environment, the ability to do time depended studies [15] and employ either laboratory equipment or state-of-the-art synchrotrons are all a very appealing evidence for the great capabilities of this non-traditional experimental approach. We believe it has all the potential to become the "standard tool" for 3D atomic structure determination in the rapidly developing field of nanoscience and technology.

Acknowledgements The work was supported by NSF through grant DMR 0304391(NIRT) and CMU through grant REF C602281. Use of the Advanced Photon Source was supported by the U. S. Department of Energy, Office of Science, Office of Basic Energy Sciences, under Contract No. DE-AC02-06CH11357.

REFERENCES

[1] Giacovazzo, C. et al, in "*Fundamentals of x-ray crystallography*", (Oxford University Press, 1998).
[2] Klug, H. P. & Alexander, L. E. in "*X-ray diffraction procedures for polycrystalline and amorphous materials*", (John Wiley & Sons, 1974).
[3] Egami, T. & Billinge, S. J. L. in "*Underneath the Bragg peaks*", (Pergamon Press, 2003).
[4] Petkov, V., Jeong, I.-K., Chung, J. S., Thorpe, M. F., Kycia, S., Billinge, S. J. L. *Phys. Rev. Lett.* **83,** 4089 (1999)
[5] Rietveld, H. M. *J Appl Crystallogr* **2,** 65 (1969).
[6] Petkov, V. *J. Appl. Crystallogr*. **22,** 387 (1989).
[7] Petkov, V., Peng, Y., Williams, G., Huang, B., Tomalia, D. and Ren, Y. *Phys. Rev. B* **72,** 19540 (2005).
[8] Petkov, V., et all. *Phys. Rev. B.* **65**, 092105 (2002).
[9] Petkov, V., Zavalij, P.Y., Lutta, S., Whittingham, M.S., Parvanov, V. & Shastri, S. *Phys. Rev. B* **69**, 085410 (2004).
[10] Tomalia, D., Naylor, A.M. & Goggard, W.A. *Angew. Chem. Int. Ed. Engl*. **29**, 138 (1990).
[11] Petkov, V., Parvanov, V., Tomalia, D., Swanson, D. Bergstrom D. & Vogt, T. *Solid State Comm.* **134**, 671 (2005).
[12] Petkov, V., Gateshki, M., Niederberger M. & Ren, Y. *Chem. Mater*. **18**, 814 (2006).
[13] Gateshki, M., Hwang, S-J., Park, D.H., Ren, Y. & Petkov, V. *Chem. Mater.* **16,** 5153 (2004).
[14] Petkov, V., Ohta, T., Hou, Y. & Ren. Y. *J. Phys. Chem.* C **111**, 714 (2007).
[15] Petkov, V., Qadir, D. & Shastri, S. *Solid State Comm*. **129**, 239 (2004).